Profiling pneumococcal type 3-derived oligosaccharides by high resolution liquid chromatography-tandem mass spectrometry

Guoyun Li[a,b], **Lingyun Li**[b], **Changhu Xue**[a], **Dustin Middleton**[f], **Robert J. Linhardt**[b,c,d,e,*], and **Fikri Y. Avci**[f,*]

[a]College of Food Science and Technology, Ocean University of China, Qingdao, Shandong 266003, China

[b]Department of Chemistry and Chemical Biology, Center for Biotechnology and Interdisciplinary Studies, Rensselaer Polytechnic Institute, Troy, NY 12180, USA

[c]Biology, Center for Biotechnology and Interdisciplinary Studies, Rensselaer Polytechnic Institute, Troy, NY 12180, USA

[d]Chemical and Biological Engineering, Center for Biotechnology and Interdisciplinary Studies, Rensselaer Polytechnic Institute, Troy, NY 12180, USA

[e]Biomedical Engineering, Center for Biotechnology and Interdisciplinary Studies, Rensselaer Polytechnic Institute, Troy, NY 12180, USA

[f]Department of Biochemistry and Molecular Biology, Center for Molecular Medicine, and Complex Carbohydrate Research Center, University of Georgia, Athens, Georgia 30602, USA

Abstract

Pneumococcal type-3 polysaccharide (Pn3P) is considered a major target for the development of a human vaccine to protect against *Streptococcus pneumonia* infection. Thus, it is critical to develop methods for the preparation and analysis of Pn3P-derived oligosaccharides to better understand its immunological properties. In this paper, we profile oligosaccharides, generated by the free radical depolymerization of Pn3P, using liquid chromatography (LC)-tandem mass spectrometry (MS/MS). Hydrophilic liquid interaction chromatography (HILIC)-mass spectrometry (MS) revealed a series of oligosaccharides with an even- and odd-number of saccharide residues, ranging from monosaccharide, degree of polymerization (dp1) to large oligosaccharides up to dp 20, generated by free radical depolymerization. Isomers of oligosaccharides with an even number of sugar residues were easily separated on a HILIC column, and their sequences could be distinguished by comparing MS/MS of these oligosaccharides and their reduced alditols. Fluorescent labeling with 2-aminoacridone (AMAC) followed by reversed phase (RP)-LC-MS/MS was applied to analyze and sequence poorly separated product mixtures, as RP-LC affords higher resolution of AMAC-

labeled oligosaccharides than does HILIC-based separation. The present methodology can be potentially applied to profiling other capsular polysaccharides.

Keywords

Pneumococcal type 3 polysaccharide; free radical depolymerization; fluorescent labeling; liquid chromatography-mass spectrometry; isomeric oligosaccharides

Introduction

Despite a long history of in-depth investigation of *Streptococcus pneumoniae*, these bacteria remain major human pathogens. Pneumococcal diseases such as pneumonia, otitis media, bacteremia, and meningitis are particularly worrisome, and oftentimes fatal to highly susceptible immunocompromised individuals, infants, and the elderly [1-3].

S. pneumoniae can be divided into over 90 serotypes based on the structural differences of the capsular polysaccharide. The capsules of these Gram-positive bacteria are considered a major virulence factor, based on the decreased virulence of non-encapsulated strains, their inability to activate the alternative complement pathway, and their resistance to phagocytosis [1]. Surface exposure of the capsular polysaccharide, and its role in the virulence capacity of *S. pneumoniae* make it an ideal candidate for vaccine development. Multiple studies have shown the ability of anti-capsular polysaccharide antibodies to provide protection from bacterial challenge [3]. A capsular polysaccharide-based vaccine (PPV23) first became available in 1983, encompassing 23 serotypes of the pneumococcus. This purely polysaccharide-based vaccine was proven effective in healthy adults, but was largely inadequate in its immunogenicity in young children. Polysaccharide-protein conjugate vaccines have been designed to enhance anti-capsular polysaccharide antibody production, [2, 3]. By coupling capsular polysaccharides to a carrier protein, a T cell dependent response is achieved along with immunoglobulin class switching, immunological memory, and rapid antibody production [4, 5]. Since the introduction of the first conjugate vaccine, PCV7, the incidence rate of pneumococcal disease has been reduced dramatically [3]. However, a global serotype distribution shift after this introduction has highlighted the importance of generating improved conjugate vaccines to include a wider range of serotypes. The current pneumococcal conjugate vaccine available is a 13-valent PCV13 (Prevnar13®), effective against the 13 most prevalent serotypes of *S. pneumoniae* [3].

By investigating the mechanism of adaptive immune activation by glycoconjugate vaccines, more effective vaccines can be thoughtfully designed. We recently characterized this mechanism, and indicated the critical role that reactive oxygen species (ROS) in the endolysosomal compartments of antigen presenting cells (APCs) has in polysaccharide processing [6]. Processed glycoconjugates are presented to T cells in the context of major histocompatibility complex type II (MHCII) molecules to initiate the adaptive immune response against the carbohydrate epitopes. A major discovery in this study was evidence of the existence of a carbohydrate-specific T cell repertoire (Tcarbs) that plays a critical role in the production of protective antibodies against the capsular polysaccharide portion of the glycoconjugate [6, 7]. We have also shown that optimizing a glycoconjugate vaccine for

these carbohydrate-specific T cell epitopes yields a robust and strong immune response and protection in a disease model [7].

Pn3P, a repeating linear co-polymer of glucuronic acid (GlcA) and glucose (Glc) (Figure 1a), was isolated from Pneumococcal type-3 (Pn3), which is considered a major target for the development of a human vaccine to protect against *S. pneumonia* infection. Pn3 is a highly virulent serotype of the pneumococcus [8]. The low efficacy of the current glycoconjugate vaccine against this capsular serotype highlights the importance of generating highly immunogenic, Pn3P-based glycoconjugate vaccines [8]. Thus, it is critical to develop methods for the preparation and analysis of Pn3P-derived oligosaccharides to better understand the immunological properties of Pn3P. Previously, small oligosaccharides containing Pn3P repeating units have been prepared either through acid hydrolysis of Pn3P [9] or synthesis [10] as there are no well-characterized enzymes available for its controlled, preparative depolymerization. In a cellular environment, reactive oxygen species are likely to degrade Pn3P in the endosomes of antigen presenting cells. Therefore, the *in vitro* free radical depolymerization used in the current study potentially mimics cellular depolymerization of Pn3P and the knowledge gained in this study should be useful for future biochemical and immunological investigations. While HILIC-FTMS and RP-FT-MS followed 2-AMAC labeling have each been previously reported in glycosaminoglycan analysis [11-17], their integrated application as a systematic strategy for profiling Pn3P, a major target for the development of a human vaccine to protect against *S. pneumonia* infection, is novel. The retention characteristics of acidic Pn3P-derived oligosaccharides on diol HILIC column and their AMAC-derivatives on C18 column are investigated. The analysis of endosomally processed Pn3P has not previously been systematically studied, and the methods developed in this study will be generally useful in the preparation of oligosaccharides to study the antigen processing mechanisms of this and other capsular polysaccharides in the endosomal compartments of APCs. In addition to describing methods for characterizing their products, this study can also inform biochemists of possible endosomal depolymerization mechanisms. Structurally defined Pn3 oligosaccharides may be useful in constructing future vaccines that are optimized for eliciting strong adaptive immune responses against the capsular polysaccharides.

2. Experimental

2.1 Materials

Pneumococcal type-3 polysaccharide (Pn3P) (Fig. 1a) was either obtained from ATCC (Manassas, VA) or purified, as described in Section *2.2*. Methanol, dimethylsulfoxide, sodium borodeuteride ($NaBD_4$), hydrogen peroxide, copper (II) acetate, acetonitrile (HPLC grade), ammonium acetate (HPLC grade), 2-aminoacridone (AMAC) (Fig. 1c), were purchased from Sigma-Aldrich (St. Louis, MO).

2.2. Purification of Pneumococcal type-3 polysaccharide

Crude bacterial extract from a capsular polysaccharide type 3 strain of *S. pneumoniae* was acquired from the laboratory of Dr. Moon Nahm at the University of Alabama at Birmingham (Birmingham, AL, USA). Purified capsular polysaccharide was obtained

through a series of enzymatic treatments and purification steps. Approximately 10 grams of the crude extract was treated with DNase (Sigma Aldrich, St. Louis, MO, USA), RNase (Sigma), and Proteinase K (Sigma) as previously described [18], followed by base treatment [19]. After extensive dialysis, the soluble polysaccharide was separated by size exclusion chromatography (Superdex 200, Sephacryl S-300, GE Healthcare) on an FPLC system (NGC Discover, Biorad). Fractions were tested for type 3 polysaccharide content in an immunoblot using type 3 specific-IgM antibody (Hyp3M6, Nahm Lab Birmingham, AL). Pooled reactive fractions were dialyzed against deionized water, and lyophilized. The purified capsular polysaccharide was obtained with a 5% yield. Purity was assayed through 1D and 2D Nuclear Magnetic Resonance Spectroscopy (Varian Inova 600 FT-NMR). The purified capsular polysaccharide of average molecular weight of >400 kDa was identical in structure and size to that obtained from the ATCC.

2.3. Preparation of Pn3P-derived oligosaccharides by free radical depolymerization

Pn3P was partially degraded through the controlled oxidative depolymerization by ROS generated using hydrogen peroxide and cupric acetate (Fig. 1a). The polysaccharide samples (200 μg) were dissolved in 100 μL 0.1 M sodium acetate-acetic acid solution containing 0.2 mM copper (II) acetate and adjusted to pH 7.0. Hydrogen peroxide (4 μL of 3% solution) was added with mixing and reacted at 45 °C for 3 h. Sodium bisulfite was added to terminate the reaction by removing excess unreacted hydrogen peroxide and the reaction mixture was divided into three portions for lyophilization. One portion of lyophilized product was dissolved in 50% acetonitrile solution (v/v) for direct HILIC-MS^n analysis. The second portion was reduced prior to analysis and the third portion was labeled with AMAC prior to analysis.

2.4 Pn3P-derived oligosaccharides reduction

Freshly prepared NaBD$_4$ reagent (20 μL of 0.05 M NaBD$_4$ in 0.01 M NaOH) was added to the freeze-dried Pn3P-derived oligosaccharides (typically 20 μg), and the reduction carried out overnight at 4 ••as previously described (Fig. 1b)[20]. The reaction solution was then neutralized to pH 7 with a solution of AcOH/H$_2$O (1:1) to destroy borohydride before passing through a 100-μL mini-column packed with cation exchange resin (AG50W-X8, H$^+$ form). After loading the sample on the column, the column was washed with 500 μL of water and the eluent solution was collected and freeze-dried. Boric acid was removed by repeated co-evaporation with MeOH.

2.5 Derivatization of Pn3P-derived oligosaccharides with AMAC

Derivatization of Pn3P-derived oligosaccharides with AMAC was performed as previously described (Fig. 1c) [21]. Briefly, the freeze-dried oligosaccharide mixture was added 20 μL a 0.1 M AMAC solution in acetic acid (AcOH)/dimethyl sulfoxide (DMSO) (3:17, v/v) and mixed by vortexing for 5 min. Next, 20 μL of 1 M NaBH$_3$CN was added in the reaction mixture and incubated at 45° C for 4 h. Finally, the AMAC-tagged oligosaccharide mixtures were analyzed by reverse-phase HPLC-Fourier transform (FT)MS^n.

2.6 HILIC LC-LTQ-Orbitrap-FT-MS Analysis of Pn3P-derived Oligosaccharides

A Luna hydrophilic interaction chromatography (HILIC) column (2.0×150 mm^2, 200 Å, Phenomenex, Torrance, CA) was used to separate mixed Pn3P-oligomers. Mobile phase A was 5 mM ammonium acetate prepared with HPLC grade water. Mobile B was 5 mM ammonium acetate prepared in 98% HPLC grade acetonitrile with 2% of HPLC grade water. After injection of 5.0 μL LMWH (2.0 μg/μL) through an Agilent 1200 autosampler, HPLC binary pump was used to deliver the gradient from 5% A to 25% A over 35 min at a flow rate of 180 μL/min. The LC column was directly connected online to the standard ESI source of LTQ-Orbitrap XL FT MS (Thermo Fisher Scientific, San-Jose, CA). The optimized parameters, used to prevent in-source fragmentation, included a spray voltage of 4.2 kV, a capillary voltage of −40 V, a tube lens voltage of −50 V, a capillary temperature of 275 °C, a sheath flow rate of 30, and an auxiliary gas flow rate of 6. External calibration of mass spectra routinely produced a mass accuracy of better than 3 ppm. All FT mass spectra were acquired at a resolution 60,000 with 300-2000 Da mass range. For the collisional induced dissociation (CID) experiments, the top 5 precursors were selected in the ion-trap with a mass window of 2.0 Da. A normalized collision energy was set to 30, and already targeted precursors were dynamically excluded for further isolation and activation for 10 s with 5 ppm tolerance for both types of analysis. The automated gain control target value at 1×10^5 in MS/MS. Product-ions were assigned using accurate mass measurement and GlycoWorkbench [22].

2.7 RP-HPLC -LTQ-Orbitrap-FT-MS Analysis of AMAC-labeled Pn3P-derived oligosaccharides

A Poroshell 120 C18 column (3.0×150 mm, 2.7 μm, Agilent, USA) was used at 45° C. Eluent A was 80 mM ammonium acetate solution and eluent B was methanol. Eluent A and 15% eluent B were flowed (150 μl/min) through the column for 5 min followed by a linear gradient from 15-30% eluent B from 5 to 30 min. The column effluent entered the electrospray ionization-MS source for continuous detection by MS^n. MS analyses were performed on LTQ-Orbitrap XL FT MS. The parameters of this instrument were set as previously described. The limit of detection (LOD) for small oligosaccharides is 0.1-1 ng but larger oligosaccharides would be expected to show a somewhat higher LOD.

2.8 Bioinformatics

Charge deconvolution was autoprocessed using DeconTools software (web source from PNNL at OMICS. PNL.GOV). The structural assignment of Pn3P-derived oligosaccharides was done by automatic processing using GlycReSoft 1.0 software developed at Boston University School of Medicine (http://code.google.com/p/glycresoft/downloads/list) [23]. For automatic processing, GlycReSoft 1.0 parameters were set as: Minimum Abundance, 1.0; Minimum Number of Scans, 1; Molecular Weight Lower Boundary, 300 Da; Molecular Weight Upper Boundary, 10000 Da; Mass Shift, ammonium; Match Error (E_M), 5.0 ppm; Grouping Error (E_G), 80 ppm; Adduct Tolerance (E_A), 5.0 ppm. For depolymerized component identification, a theoretical database was generated by GlycReSoft 1.0 for different structures. The quantitative data were normalized to the total identified oligosaccharides peak area (in the format of percentage, %). Mass spectra were annotated

with GlycoWorkbench software [22]. Briefly, the mass spectra were opened in GlycoWorkbench, and peaks were annotated with all possible structures for a given ion. The annotation was used a guide to determine the possible fragment-ions observed in MS/MS analyses, nomenclature used to define the fragmentation is based on that introduced by Domon and Costello [24].

3. Results and discussion

3.1 Pn3P-derived Oligosaccharides preparation and HILIC-MS/MS analysis

Reactive oxygen species (ROS), generated through the use of chemical reagents and radiation have been widely used to depolymerize polysaccharides and sulfated polysaccharides [11,12,25]. The hydroxyl radical, the most reactive ROS, can abstract hydrogen atoms at ring C – H bonds of aldoses, uronic acids, and other sites on carbohydrates except for the C-2 of N-acetyl hexosamine residues [26,27]. The abstraction of hydrogen atom generates carbon-centered radicals. Radicals at the carbons forming glycosidc bonds undergo a β-scission reaction resulting in the breakdown of polysaccharide chains into oligosaccharides [26-28]. Therefore, ROS-based depolymerization affords relatively non-selective fragmentation a wide variety of polysaccharides. ROS-based depolymerization represents an important route for polysaccharide degradation because of its reproducibility, constant composition, and for the easy control of the extent of depolymerization. Recently, ROS generated using ferrous ion and hydrogen peroxide was used in our laboratory to depolymerize hyaluronan into oligosaccharides that could be characterized by LC-MS [25]. Using this same approach we tested the sensitivity of Pn3P to ROS-based depolymerization. Hydroxyl free radical-mediated, controlled depolymerization of Pn3P using copper (II) and hydrogen peroxide at pH 7.0 afforded oligosaccharides for analysis by LC-MS. Separation of oligosaccharides before mass spectrometry is essential for comprehensive oligosaccharide profiling owing to the complexity of the product mixtures. Moreover, MS allows high sensitivity detection of the oligosaccharides formed [21]. Some notable success in separation of oligosaccharides has been achieved through using HILIC [13,29,30], which was based on analyte polarity and affords good separation of glycans, especially for the isomers [12]. The Luna HILIC column, relying on a cross-linked diol solid-phase support, instead of the standard amide support, was applied after surveying a number of HILIC chemistry [31]. The high-resolution and high mass accuracy of ESI-FTMS makes this method suitable for glycan analysis.

The raw data from the HILIC LC-FTMS was deconvoluted using DeconTools, and then, the output of DeconTools was processed by GlycResoft to generate matching structures and to provide quantitative information [23]. Quantitative results on the major oligosaccharides are shown in Fig. 2. Twenty-eight oligosaccharide compositions were matched by GlycResoft including from degree of polymerization (dp) 2 to dp20 oligosaccharides including even-and odd-chain oligosaccharides. Approximately 90% of the oligosaccharides had a size of < dp 12. The oligosaccharides observed included [n residues GlcA n, Glc residues], n = 1-9), [n GlcA residues, n+1 Glc residues], and [n+1 GlcA residues, n Glc residues]. The degree of polymerizations (dp 2 to 20) of these oligosaccharides were extracted from the chromatography of HILIC-MS analysis data (Fig. 3a) based on a mass accuracy of < 5 ppm.

For oligosaccharides with an odd-number of sugar residues of the same dp, the [n, n+1] oligosaccharide with lower polarity eluted first, followed by the [n+1, n] oligosaccharide. These two groups of oligosaccharides could be completely separated only when the n was 4. Most of the oligosaccharides with an even number of sugar residues showed a double peak, corresponding to two isomers, one with a GlcA located the reducing-end of the chain (GlcA$_{re}$) and one having a Glc located the reducing-end of the chain (Glc$_{re}$). Only the isomer pairs of dp2, dp4 and dp6 were well separated on the HILIC column.

LC-MS/MS analysis of the oligosaccharide mixtures was carried out to further confirm elution order of the oligosaccharides with an even number of sugar residues. The sequences of these oligosaccharides could not be distinguished from their MS/MS spectra, which all show the same product-ions but in different abundances. Therefore, the product mixture was reduced with NaBD$_4$ (Fig. 1b) prior to analysis by HILIC-MS/MS analysis. The MS/MS data were then annotated using GlycoWorkbench Software [22]. The reducing-end terminal fragment-ions showed an increase of 3 mass units after the reduction reaction. The MS/MS spectra of Pn3P-derived disaccharides (m/z = 355.09) and its reduced alditol (m/z = 358.11) are shown in Fig. 4. Three product ions m/z 178.10, 196.03, and 340.25 showed 3 mass unit shift in the MS/MS spectrum of Peak H1 (Fig. 3a, dp2) and these were assigned as Z$_1$, Y$_1$ and [M-H$_2$O]$^-$ (Fig. 4a). Therefore, the sequence of peak H1 was [1, 1]GlcA$_{re}$ (Table 1). Similarly, the product ion m/z 164.03(Z$_1$), 182.17 (Y$_1$) and 340.09 ([M-H$_2$O]$^-$) in the Fig. 4d suggested the sequence of peak H2 was [1, 1]Glc$_{re}$. Comparing the MS/MS spectra of oligomers and their reduced alditols (Fig. S1 and Fig. S2) allowed us to confirm that the sequences of peak H5, H6, H9 and H10 (Fig. 3a, dp4 and dp6) were [2, 2]GlcA$_{re}$, [2, 2]Glc$_{re}$, [3, 3]GlcA$_{re}$ and [3, 3]Glc$_{re}$, respectively. In conclusion, the even numbers of Pn3P-derived oligosaccharides with GlcA located in the reducing-end eluted first from the HILIC column. The detailed separation and sequence information are provided in Table 1. In Fig. 2a, it was observed that the size of the oligosaccharide (dp) is the critical factor affecting the retention of Pn3P-oligosaccharides on the HILIC column. The retention of the oligosaccharides increased with their size raising. The linkage and the number of GlcA could affect the different oligomers in the same dp number. All the effects were decreased as the chains of oligomers increased, until the oligomers were shown in one peak.

3.2 Derivatization of Pn3P-derived oligosaccharides with 2-aminoacridone and RP-HPLC - LTQ-Orbitrap-FT-MS Analysis

The chromatographic properties in RP-HPLC can be improved by labeling the oligosaccharides with the hydrophobic fluorophore. The AMAC-labelled different isomers of glycosaminoglycan-derived disaccharides had a good separation on C18 column [15]. The sequences of larger Pn3P-derived oligosaccharides with even number of sugar residues were not easily confirmed because it was not possible to identify the reducing-end through its reduction. Modifications of the reducing-ends, of the Pn3P-derived oligosaccharides, were next labeled through their reductive amination with AMAC (Fig. 1c), and the RP-HPLC-FT-MSMS analysis was performed. Based on a mass accuracy of < 5 ppm, AMAC-labeled oligosaccharides of dp1 to 20 were extracted and shown in Fig. 3b. Monosaccharides, R$_1$ and R$_2$ (Fig. 3b, dp1) were assigned to AMAC-labeled glucose (Glc-AMAC) and glucuronic acid (GlcA-AMAC) for the m/z 373.14 and 387.12, respectively.

Their MS/MS spectrum (Fig. S3) shows specific productions of m/z 277.12, 355.28 for Glc-AMAC and m/z 369.16 for GlcA-AMAC. These data simplify the sequence identification of oligosaccharides having an even-number of sugar residues. The separation of AMAC-labeled Pn3P-derived oligosaccharides, however, was very complicated, especially for the even numbers of oligosaccharides. As shown in Fig. 3b, the same odd dp (up to dp19) number of AMAC-labeled oligosaccharide were well separated but showed three peaks. According to the mass of AMAC-labeled oligosaccharides with an odd-number of sugar units, the [n+1, n]GlcA$_{re}$-AMAC eluted first with two peaks. The [n, n+1]Glc$_{re}$-AMAC next eluted from the reverse-phase column. The AMAC-labeled oligosaccharides with an even number of sugar units afforded complicated MS/MS data (not shown) indicating that the AMAC-labeled isomers of dp2 and dp4 were not completely separated, while the isomers of dp 6 were separated and the [n, n]GlcA$_{re}$-AMAC eluted earlier than [n, n]Glc$_{re}$-AMAC (n 3). The detailed separation and sequence information are provided in Table 2. The retention times for [n, n]Glc$_{re}$-AMAC, [n, n+1]Glc$_{re}$-AMAC and one peak of [n, n-1]GlcA$_{re}$-AMAC are almost identical. Therefore, the number of GlcA residues in each oligosaccharide represents a critical factor affecting the retention of AMAC-labeled Pn3P-derived oligosaccharides.

3.3 Effect of 2-aminoacridone derivatization for the MS/MS spectrum of Pn3P-derived oligosaccharides

The derivatization of oligosaccharides using reductive amination can influence fragmentation patterns of oligosaccharides producing fewer internal cleavage-ions and, thus, simplifying structural analysis [32,33]. Therefore, the MS/MS spectra of Pn3P-hexasaccharides and AMAC-labeled hexasaccharides were compared (Fig. 5). Since cleavage products from both the reducing-end and the nonreducing-end can produce the same fragments, it is often difficult to assign a peak to a particular fragment. The MS/MS spectrum with [M-2H]$^{2-}$ of underivatized Pn3P-derived hexasaccharides (m/z 515.12) and its reduced alditol (m/z 516.63) as precursor-ions are shown in Fig. S2. The sequences of isomeric hexasaccharides were confirmed by the comparison with the MS/MS of its reduced alditol as discussed above. The cleavage of the isomer's MS/MS spectra, results in prominent C- and Y-ions afforded by cleaving the glycosidic linkage of GlcA(1-4)Glc, Y_5 to [3, 3]Glc$_{re}$ and Y_4 to [3, 3]GlcA$_{re}$. Furthermore, some abundant cross-ring cleavage-ions, $^{0,2}A_n$ and the same fragment with water loss were formed. The $^{0,2}A_n$ fragmentation on the reducing end has been produced by the mechanism for its occurrence postulated by a reducing end retro-aldol rearrangement pathway [13,34]. Decarboxylated ions and fragments with water loss were also produced.

The MS/MS spectra with [M-2H]$^{2-}$ of AMAC-labeled Pn3P-derived isomeric hexasaccharides (m/z 612.17) are shown in Fig. 5. The fragment ions 355.13/373.20 (Fig. 5a) and 369.17/387.26 (Fig. 5b) indicated the monosaccharide residues at the reducing-end of these two oligosaccharides were Glc and GlcA, respectively. Abundant Y-/B-ions were formed in the mass spectra, especially those that were also most prominent from the glycosidic bond cleavages of GlcA(1-4)Glc. The Y_1/B_5, Y_3/B_3 and Y_5 were the most abundant ions formed in the mass spectra of [3, 3]Glc$_{re}$-AMAC (Fig. 5a). The major fragment ions of [3, 3]GlcA$_{re}$-AMAC correspond to Y_4 and Y_2/B_4. Therefore, the reductive

amination of oligosaccharides promoted the formation of Y-/B-ions, giving a very simple fragmentation pattern from which the oligosaccharide's sequence can easily be deduced. Weak cross-ring fragments were also observed and the main fragments were $^{0,2}A_n$ ions. Some other minor cross-ring cleavage ions were also formed which are informative for the linkages of monosaccharide residues constituting these oligosaccharides. The presence of the $^{3,5}X_4$ ion at 812.33 in Fig. 5b allows the identification of the 1→4 linkage between the GlcA residue and the Glc residue. The m/z 633.31 ($^{0,2}A_4$) and 559.10 ($^{1,3}A_4$) reveals that the linkage between Glc and GlcA is 1-3 glycosidic linkage. Nonetheless, the abundance of the cross-ring fragments was still limited. High collision energy applied in the mass experiment or multi-stage mass spectra might improve this and will be the object in further studies.

4. Conclusions

This study demonstrates that ROS-based depolymerization of Pn3P affords oligosaccharides, and even and odd number of sugar residues, ranging in size from dp1 to dp20. These oligosaccharides could be separated using HILIC or by RP-LC following their reductive amination with AMAC. The size and composition of these oligosaccharides could be established through their elution position and through the use of FTMS analysis and their sequence could be deduced using MS/MS analysis. The retention characteristics of Pn3P-derived oligosaccharides and their AMAC-derivatives on HILIC and C18 column, respectively, were elaborated. The size of the oligosaccharides was the critical factor in their retention on the HILIC column. The linkage and the number of acidic sugar residues were secondary factors. The number of acidic sugar residues plays a more important role in the retention of AMAC-labeled oligosaccharides on the reverse phase column than their size. These studies will be useful in the separation of unknown oligosaccharides in LC-MS analysis. While quantification is particularly problematic using MS detection allowing semi-quantification by normalization of the abundance from bioinformatics software, it is possible to accurately quantify AMAC-labeled oligosaccharides using fluorescence detection. The present research strategies could be potentially applied to profiling other capsular polysaccharides.

Supplementary Material

Refer to Web version on PubMed Central for supplementary material.

Acknowledgments

References

1. Alonso DeValesco E, Verheul AFM, Vernhoef J, Snippe H. Streptococcus pneumoniae: virulence factors, pathogenesis, and vaccines. Microbiol Rev. 1995; 59:591–603. [PubMed: 8531887]

2. Grabenstein JD, Klugman KP. A century of pneumococcal vaccination research in humans. Clin Microbiol Infec. 2012; 18:15–24. [PubMed: 22882735]

3. Torres A, Bonanni P, Hryniewicz W, Moutschen M, Reinert RR, Welte T. Pneumococcal vaccination: what have we learnt so far and what can we expect in the future? Eur J Clin Microbiol Infect Dis. 2015; 34:19–31. [PubMed: 25149825]

4. Avci FY, Kasper DL. How bacterial carbohydrates influence the adaptive immune system. Annu Rev Immunol. 2010; 28:107–130. [PubMed: 19968562]

5. Avci FY. Novel strategies for development of next-generation glycoconjugate vaccines. Curr Top Med Chem. 2013; 13:2535–2540. [PubMed: 24066893]

6. Avci FY, Li X, Tsuji M, Kasper DL. A mechanism for glycoconjugate vaccine activation of the adaptive immune system and its implications for vaccine design. Nat Med. 2011; 17:1602–1609. [PubMed: 22101769]

7. Avci FY, Li X, Tsuji M, Kasper DL. Isolation of carbohydrate-specific CD4$^+$ T cell clones from mice after stimulation by two model glycoconjugate vaccines. Nat Protoc. 2012; 7:2180–2192. [PubMed: 23196974]

8. Demczuk W, Martin I, Griffith A, Lefebvre B, McGeer A, Lovgren M, Tyrrell G, Desai S, Sherrard L, Adam H, Gilmour M, Zhanel G. Serotype distribution of invasive *Streptococcus pneumoniae* in Canada after the introduction of the 13-valent pneumococcal conjugate vaccine, 2010–2012. Can J Microbiol. 2013; 59:778–788. [PubMed: 24313450]

9. Lefeber DJ, Gallego RG, Grun CH, Proietti D, D'Ascenzi S, Costantino P, Kamerling JP, Vliegenthart JFG. Isolation of oligosaccharides from a partial-acid hydrolysate of pneumococcal type 3 polysaccharide for use in conjugate vaccines. Carbohydr Res. 2002; 337:819–825. [PubMed: 11996835]

10. Lefeber DJ, Arévalo EA, Kamerling JP, Vliegenthart JFG. Synthesis of a hexasaccharide fragment of the capsular polysaccharide of *Streptococcus pneumoniae* type 3. Can J Chem. 2002; 80:76–81.

11. Li G, Masuko S, Green DE, Xu Y, Li L, Zhang F, Xue C, Liu J, DeAngelis PL, Linhardt RJ. *N*-Sulfotestosteronan, A novel substrate for heparan sulfate *6-O*-sulfotransferases and its analysis by oxidative degradation. Biopolymers. 2013; 99:675–685. [PubMed: 23606289]

12. Li G, Cai C, Li L, Fu L, Chang Y, Zhang F, Toida T, Xue C, Linhardt RJ. New contaminant in heparin and determination by radical depolymerization and liquid chromatography-mass spectrometry. Anal Chem. 2014; 86:326–330. [PubMed: 24364596]

13. Li L, Zhang F, Zaia J, Linhardt RJ. Top-down approach for the direct characterization of low molecular weight heparins using LC-FT-MS. Anal Chem. 2012; 84:8822–8829. [PubMed: 22985071]

14. Hofmeister GE, Zhou Z, Leary JA. Linkage position determination in lithium-cationized disaccharides: tandem mass spectrometry and semiempirical calculations. J Am Chem Soc. 1991; 113:5964–5970.

15. Volpi N, Galeotti F, Yang B, Linhardt RJ. Analysis of glycosaminoglycan-derived, precolumn, 2-aminoacridone-labeled disaccharides with LC-fluorescence and LC-MS detection. Nat Protoc. 2014; 9:541–558. [PubMed: 24504479]

16. Karlsson NG, Schulz BL, Packer NH, Whitelock JM. Use of graphitised carbon negative ion LC-MS to analyse enzymatically digested glycosaminoglycans. J Chromatogr B. 2005; 824:139–47.

17. Huang R, Liu J, Sharp JS. An approach for separation and complete structural sequencing of heparin/heparan sulfate like oligosaccharides. Anal Chem. 2013; 85:5787–5795. [PubMed: 23659663]

18. Michon F, Katzenellenbogen E, Kasper DL, Jennings HJ. Structure of the complex group-specific polysaccharide of group B Streptococcus. Biochemistry. 1987; 26:476–86. [PubMed: 3548820]

19. Choi YH, Roehrl MH, Kasper DL, Wang JY. A unique structural pattern shared by T-cell-activating and abscess-regulating zwitterionic polysaccharides. Biochemistry. 2002; 41:15144–15151. [PubMed: 12484751]

20. Yang B, Yu G, Zhao X, Jiao G, Ren S, Chai W. Mechanism of mild acid hydrolysis of galactan polysaccharides with highly ordered disaccharide repeats leading to a complete series of exclusively odd-numbered oligosaccharides. FEBS J. 2009; 276:2125–2137. [PubMed: 19292880]

21. Yang B, Chang Y, Weyers AM, Sterner E, Linhardt RJ. Disaccharide analysis of glycosaminoglycan mixtures by ultra-high-performance liquid chromatography–mass spectrometry. J Chromatogr A. 2012; 1225:91–98. [PubMed: 22236563]

22. Ceroni A, Maass K, Geyer H, Geyer R, Dell A, Haslam SM. GlycoWorkbench: A tool for the computer-assisted annotation of mass spectra of glycans. J Proteome Res. 2008; 7:1650–1659. [PubMed: 18311910]

23. Maxwell E, Tan Y, Tan Y, Hu H, Benson G, Aizikov K, Conley S, Staples GO, Slysz GW, Smith RD, Zaia J. GlycReSoft: A software package for automated recognition of glycans from LC/MS data. PloS one. 2012; 7:e45474. [PubMed: 23049804]

24. Domon B, Costello CE. A systematic nomenclature for carbohydrate fragmentations in FAB-MS/MS spectra of glycoconjugates. Glycoconjugate J. 1988; 5:397–409.

25. Zhao X, Yang B, Li L, Zhang F, Linhardt RJ. On-line separation and characterization of hyaluronan oligosaccharides derived from radical depolymerization. Carbohydr Polym. 2013; 96:503–509. [PubMed: 23768593]

26. Gilbert BC, King DM, Thomas B. Radical reactions of carbohydrates. Part 2. An electron spin resonance study of the oxidation of D-glucose and related compounds with the hydroxyl radical. J Chem Soc Perkin Trans. 1981; 2:1186–1199.

27. Hawkins CL, Davies MJ. Degradation of hyaluronic acid, poly- and mono-saccharides, and model compounds by hypochlorite: Evidence for radical intermediates and fragmentation. Free Radic Biol Med. 1998; 24:1396–1410. [PubMed: 9641257]

28. Rees MD, Kennett EC, Whitelock JM, Davies MJ. Oxidative damage to extracellular matrix and its role in human pathologies. Free Radic Biol Med. 2008; 44:1973–2001. [PubMed: 18423414]

29. Karlsson G, Swerup E, Sandberg H. Combination of two hydrophilic interaction chromatography methods that facilitates identification of 2-aminobenzamide-labeled oligosaccharides. J Chromatogr Sci. 2008; 46:68–73. [PubMed: 18218191]

30. Leijdekkers AGM, Sanders MG, Schols HA, Gruppen H. Characterizing plant cell wall derived oligosaccharides using hydrophilic interaction chromatography with mass spectrometry detection. J Chromatogr A. 2011; 1218:9227–9235. [PubMed: 22099219]

31. Fu Q, Liang T, Li Z, Xu X, Ke Y, Liang X. Separation of carbohydrates using hydrophilic interaction liquid chromatography. Carbohydr Res. 2013; 379:13–17. [PubMed: 23835469]

32. Shen X, Perreault HJ. Investigation of different combinations of derivatization, separation methods and electrospray ionization mass spectrometry for standard oligosaccharides and glycans from ovalbumin. J Mass Spectrom. 2001; 36:563–574. [PubMed: 11391813]

33. Morelle W, Slomianny MC, Diemer H, Schaeffer C, van Dorsselaer A, Michalski JC. Structural characterization of 2-aminobenzamide-derivatized oligosaccharides using a matrix-assisted laser desorption/ionization two-stage time-of-flight tandem mass spectrometer. Rapid Commun Mass Spectrom. 2005; 19:2075–2084. [PubMed: 15988715]

34. Saad OM, Leary JA. Delineating mechanisms of dissociation for isomeric heparin disaccharides using isotope labeling and ion trap tandem mass spectrometry. J Am Soc Mass Spectrom. 2004; 15:1274–1286. [PubMed: 15337508]

Highlights

- Pneumococcal type 3 polysaccharide (PnP3) is depolymerized

- Pn3P derived oligosacchides are separated by liquid chromatography (LC).

- Hydrophilic interaction LC and reverse phase LC are used in their separation.

- LC-mass spectrometry (MS) analysis determined oligosaccharide composition.

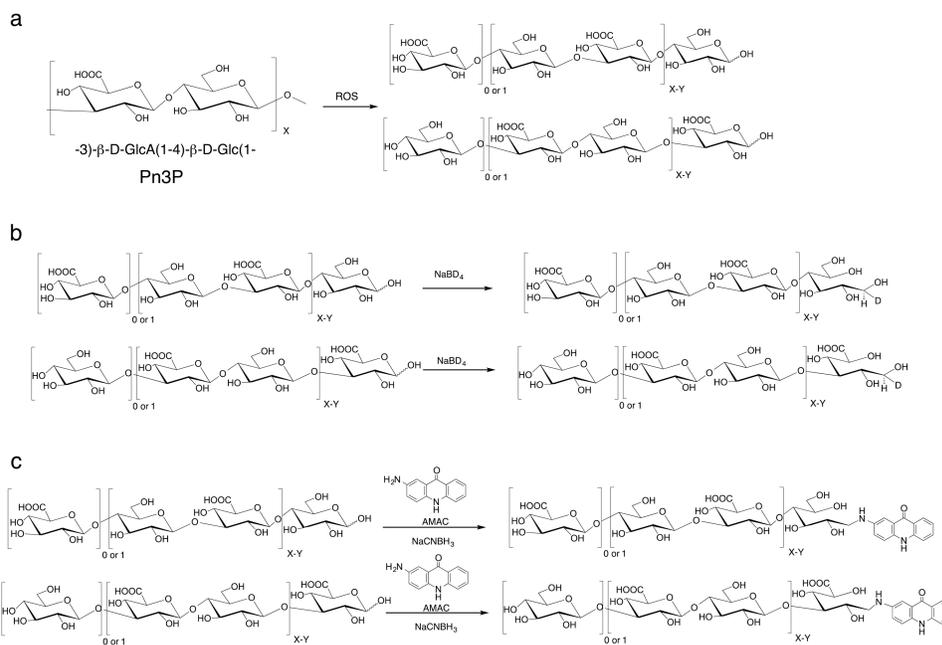- LC-tandem MS analysis determined oligosaccharide sequence

Fig. 1.
Pneumococcal type-3 polysaccharide (Pn3P) structure, its depolymerization through treatment with reactive oxygen species (ROS) and the modifications of the resulting oligosaccharides by reduction and reductive amination (a) The repeating unit structure of Pn3P and its depolymerization using ROS. X = number of repeating units, X-Y = number of repeating units reduced by Y units following depolymerization reaction. (b) Reduction and deuterium labeling of reaction of Pn3P-derived oligosaccharides, (c) 2-aminoacridone (AMAC) labeling of Pn3P-derived oligosaccharides by reductive amination
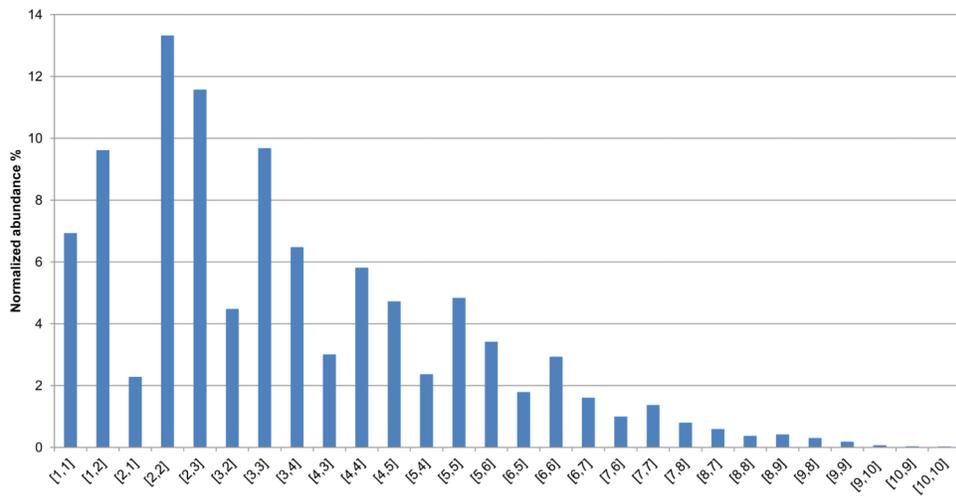
Fig. 2.
Quantitative distribution of Pn3P-derived oligosaccharides prepared by Pn3P depolymerization using ROS. The bar graph shows the normalized abundance of oligosaccharides comprised of [residues of GlcA, residues of Glc].
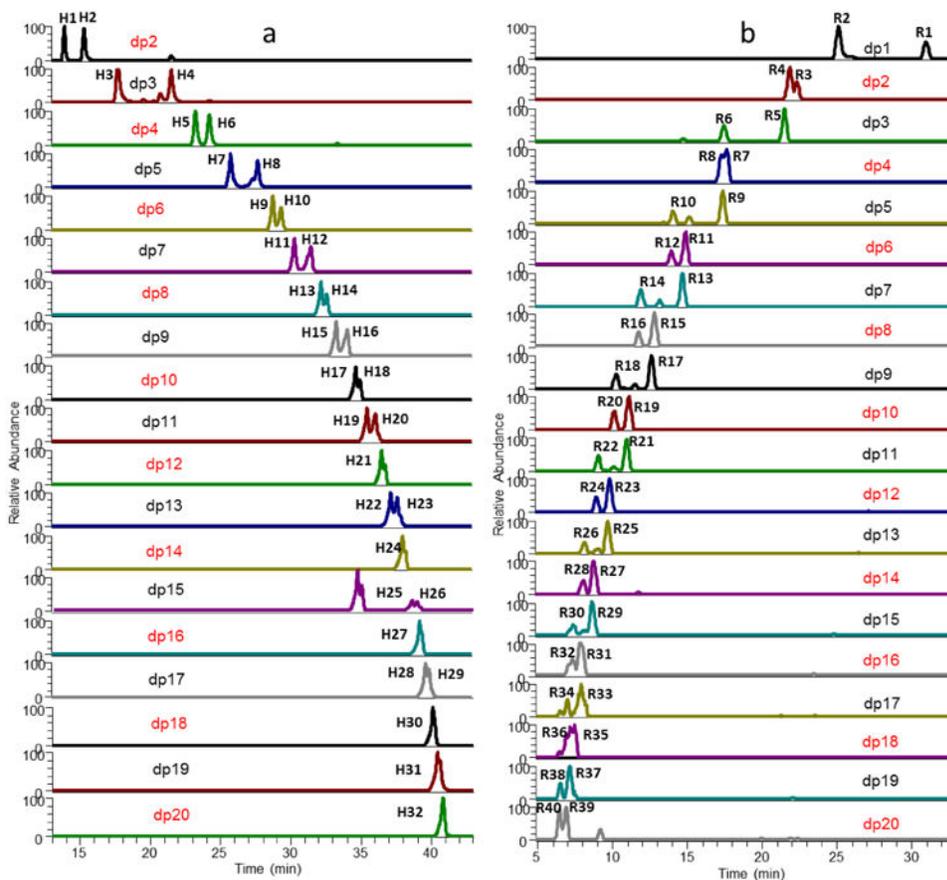
Fig. 3.
The extracted ion chromatograms (EICs) Pn3P-derived oligosaccharides and AMAC-labeled Pn3P-derived oligosaccharides analyzed by LC-MS. (a) EICs of Pn3P-derived oligosaccharides based on HILIC-MS analysis. (b) EICs of AMAC-labeled Pn3P-derived oligosaccharides based on RP-HPLC-MS analysis.
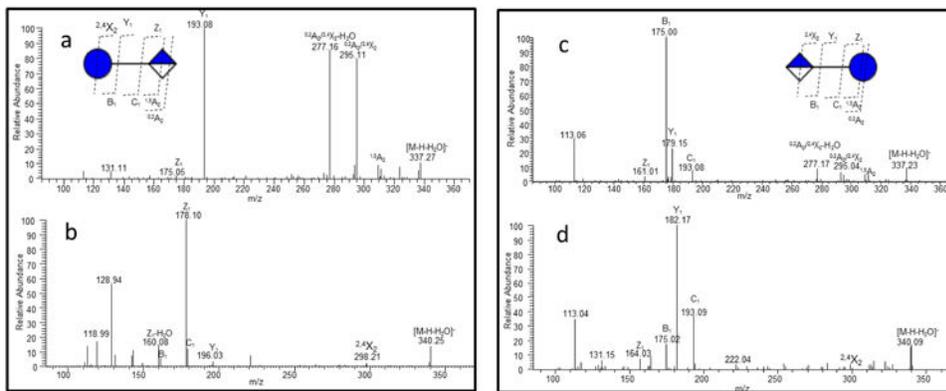
Fig. 4.

MS/MS spectrum of Pn3P-derived disaccharides (m/z = 355.09) from radical depolymerization of Pn3P and its reduced alditol (m/z = 358.11). (a) Peak H1, (b) Peak H2. Symbols identifying sugar residues are as follows: (●) glucose; (◆) glucuronic acid.

Fig. 5.
MS/MS spectrum of Pn3P-derived hexasaccharides labeled by AMAC (m/z = 612.17). (a) MS/MS of peak R11 in Fig. 3b, dp6, (b) MS/MS of peak R12 in Fig. 3b, dp6. Symbols identifying sugar residues are as follows: (●) glucose; (◇) glucuronic acid.

Table 1

Retention time (t_R,min) and resolution of oligosaccharides obtained from radical depolymerization of PnP3 analyzed by HILIC-MS analysis

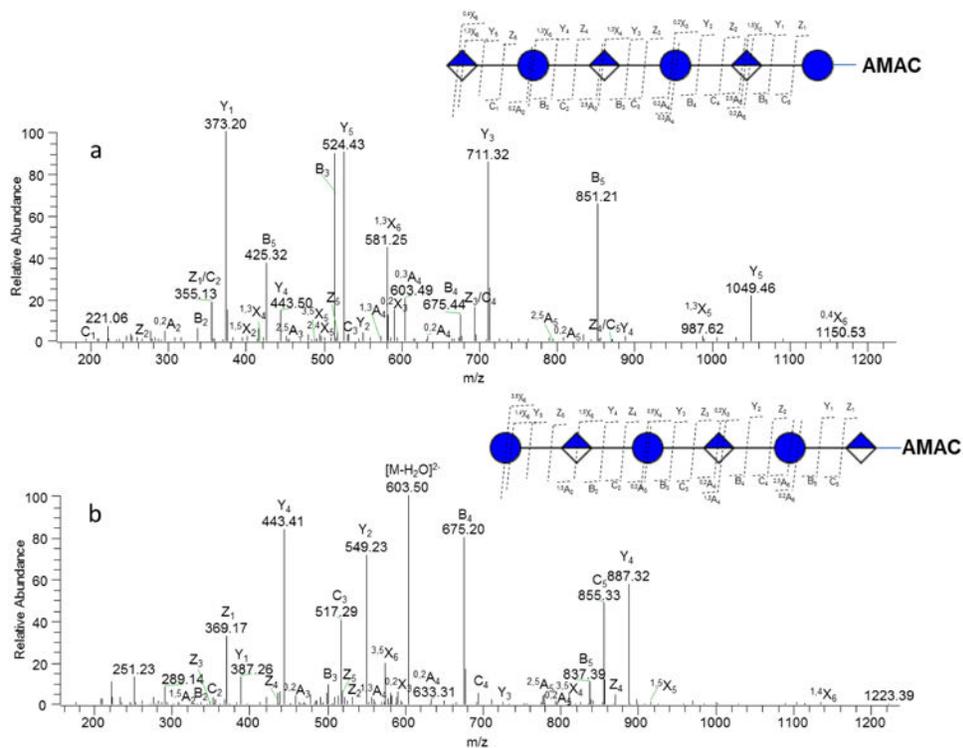| Peak number	t_R (min)	Resolution	dp	Suggested sequence
1	14.98	—	2	[1,1]GlcA$_{re}$ [*]
2	16.43	2.17	2	[1,1]Glc$_{re}$
3	18.85	3.83	3	[1,2]Glc$_{re}$
4	22.70	6.33	3	[2,1]GlcA$_{re}$
5	24.42	3.00	4	[2,2]GlcA$_{re}$
6	25.40	1.67	4	[2,2]Glc$_{re}$
7	26.91	2.33	5	[2,3]Glc$_{re}$
8	28.89	3.33	5	3,2]GlcA$_{re}$
9	29.97	1.83	6	[3,3]GlcA$_{re}$
10	30.56	1.17	6	[3,3]Glc$_{re}$
11	31.53	1.67	7	[3,4]Glc$_{re}$
12	32.76	2.17	7	[4,3]GlcA$_{re}$
13	33.50	1.33	8	[4,4]GlcA$_{re}$
14	33.92	-[**]	8	[4,4]Glc$_{re}$
15	34.60	1.17	9	[4,5]Glc$_{re}$
16	35.41	-	9	[5,4]GlcA$_{re}$
17	36.06	-	10	[5,5]GlcA$_{re}$
18	36.32	-	10	[5,5]Glc$_{re}$
19	36.84	-	11	[5,6]Glc$_{re}$
20	37.42	-	11	[6,5]GlcA$_{re}$
21	37.93	-	12	[6,6]GlcA$_{re}$, [6,6]Glc$_{re}$
22	38.60	-	13	[6,7]Glc$_{re}$
23	39.05	-	13	[7,6]GlcA$_{re}$
24	39.38	-	14	[7,7]GlcA$_{re}$, [7,7]Glc$_{re}$
25	39.90	-	15	[7,8]Glc$_{re}$
26	40.20	-	15	[8,7]GlcA$_{re}$
27	40.44	-	16	[8,8]GlcA$_{re}$, [8,8]Glc$_{re}$
28	40.82	-	17	[8,9]Glc$_{re}$
29	41.00	—	17	[9,8]GlcA$_{re}$
30	41.21	-	18	[9,9]GlcA$_{re}$, [9,9]Glc$_{re}$
31	41.52	-	19	[10,9]GlcA$_{re}$, [9,0]Glc$_{re}$
32	41.84	-	20	[10,0]GlcA$_{re}$, [10,0]Glc$_{re}$

[*] Oligosaccharide compositions are given as [GlcA,Glc]X$_{re}$, X$_{re}$ is the sugar residue located in the reducing end.

[**] "-" means that the resolution of the oligosaccharide compared with the former was less than 1.0.

Table 2

Retention time (tR,min) and resolution of oligosaccharides obtained from enzymatic radical depolymerization of PnP3 analyzed by RP-HPLC-MS analysis (retention time sequence)

Peak number	tR (min)	Resolution	dp	Suggested sequence
1	31.14	—	1	[0,1]Glc$_{re}$ -AMAC*
2	25.28	6.51	1	[1,0]GlcA$_{re}$ -AMAC
3	22.52	3.25	2	[1,1]GlcA$_{re}$ -AMAC
4	22.02	-	2	[1,1]Glc$_{re}$ -AMAC
5	21.68	-	3	[1,2]Glc$_{re}$ -AMAC
6	17.64	6.73	3	[2,1]GlcA$_{re}$ -AMAC
7	17.81	-	4	[2,2]Glc$_{re}$ -AMAC
8	17.47	-	4	[2,2]GlcA$_{re}$ -AMAC
9	17.55	-	5	[2,3]Glc$_{re}$ -AMAC
10	14.21, 15.33	3.70	5	[3,2]GlcA$_{re}$ -AMAC
11	15.09	-	6	[3,3]Glc$_{re}$ -AMAC
12	14.10	1.65	6	[3,3]GlcA$_{re}$ -AMAC
13	14.86	-	7	[3,4]Glc$_{re}$ -AMAC
14	12.08, 13.34	2.76	7	[4,3]GlcA$_{re}$ -AMAC
15	12.99	-	8	[4,4]Glc$_{re}$ -AMAC
16	11.91	1.80	8	[4,4]GlcA$_{re}$ -AMAC
17	12.79	-	9	[4,5]Glc$_{re}$ -AMAC
18	10.43, 11.67	1.87	9	[5,4]GlcA$_{re}$ -AMAC
19	11.31	-	10	[5,5]Glc$_{re}$ -AMAC
20	10.30	1.68	10	[5,5]GlcA$_{re}$ -AMAC
21	11.14	-	11	[5,6]Glc$_{re}$ -AMAC
22	9.23, 10.26	1.47	11	[6,5]GlcA$_{re}$ -AMAC
23	9.98	-	12	[6,6]Glc$_{re}$ -AMAC
24	9.10	1.47	12	[6,6]GlcA$_{re}$ -AMAC
25	9.85	-	13	[6,7]Glc$_{re}$ -AMAC
26	8.27, 9.19	1.20	13	[7,6]GlcA$_{re}$ -AMAC
27	8.91	-	14	[7,7]Glc$_{re}$ -AMAC
28	8.25	1.32	14	[7,7]GlcA$_{re}$ -AMAC
29	8.83	-	15	[7,8]Glc$_{re}$ -AMAC
30	7.55, 8.45	-	15	[8,7]GlcA$_{re}$ -AMAC
31	8.02	-	16	[8,8]Glc$_{re}$ -AMAC
32	7.51	-	16	[8,8] GlcA$_{re}$ -AMAC
33	7.90	-	17	[8,9]Glc$_{re}$ -AMAC
34	7.01	-	17	[9,8]GlcA$_{re}$ -AMAC

Peak number	tR (min)	Resolution	dp	Suggested sequence
35	7.47	-	18	$[9,9]Glc_{re}$ -AMAC
36	6.93	-	18	$[9,9]GlcA_{re}$ -AMAC
37	7.15	-	19	$[9,0]Glc_{re}$ -AMAC
38	6.52	-	19	$[10,9]GlcA_{re}$ -AMAC
39	6.91	-	20	$[10,0]Glc_{re}$ -AMAC
40	6.49	-	20	$[10,0]GlcA_{re}$ -AMAC

*
AMAC-labeled oligosaccharide conjugate compositions are given as $[GlcA,Glc]X_{re}$-AMAC, X_{re} is the sugar residue located in the reducing end.

**
"-" means that the resolution of the oligosaccharide compared with the former was less than 1.0.